2012

Selective Oma1 Protease-mediated Proteolysis of Cox1 Subunit of Cytochrome Oxidase in Assembly Mutants

Oleh Khalimonchuk
University of Nebraska-Lincoln, okhalimonchuk2@unl.edu

Mi-Young Jeong
University of Utah Health Sciences Center

Talina Watts
University of Utah Health Sciences Center

Elliott Ferris
University of Utah Health Sciences Center

Dennis R. Winge
University of Utah Health Sciences Center

THE JOURNAL OF BIOLOGICAL CHEMISTRY VOL. 287, NO. 10, pp. 7289–7300, March 2, 2012

Selective Oma1 Protease-mediated Proteolysis of Cox1 Subunit of Cytochrome Oxidase in Assembly Mutants*

Received for publication, October 12, 2011, and in revised form, January 2, 2012 Published, JBC Papers in Press, January 4, 2012, DOI 10.1074/jbc.M111.313148

Oleh Khalimonchuk, Mi-Young Jeong, Talina Watts, Elliott Ferris, and Dennis R. Winge[1]

From the Departments of Medicine and Biochemistry, University of Utah Health Sciences Center, Salt Lake City, Utah 84132

Background: Yeast lacking Coa2 are deficient in cytochrome *c* oxidase due to Cox1 degradation.
Results: Oma1 mediates Cox1 degradation in *coa2*Δ cells but not other mutants stalled in oxidase biogenesis.
Conclusion: Impaired hemylation of Cox1 in *coa2*Δ cells leads to misfolding and facile degradation by Oma1.
Significance: Oma1 functions in quality control of cytochrome oxidase assembly.

Stalled biogenesis of the mitochondrial cytochrome *c* oxidase (CcO) complex results in degradation of subunits containing redox cofactors. The conserved Oma1 metalloproteinase mediates facile Cox1 degradation in cells lacking the Coa2 assembly factor, but not in a series of other mutants stalled in CcO maturation. Oma1 is activated in *coa2*Δ cells, but the selective Cox1 degradation does not arise merely from its activation. Oma1 is also active in cells with dysfunctional mitochondria and *cox11*Δ cells impaired in CcO maturation, but this activation does not result in Oma1-mediated Cox1 degradation. The facile and selective degradation of Cox1 in *coa2*Δ cells, relative to other CcO assembly mutants, is likely due to impaired hemylation and subsequent misfolding of the subunit. Specific Cox1 proteolysis in *coa2*Δ cells arises from a combination of Oma1 activation and a susceptible conformation of Cox1.

Cytochrome *c* oxidase (CcO,[2] complex IV) is the terminal enzyme of the energy transducing respiratory chain in mitochondria. Eukaryotic CcO consists of 12–13 subunits, with three mitochondrial encoded subunits (Cox1–Cox3) forming the core enzyme with the redox copper and heme cofactors (1). The remaining nuclear encoded subunits form the periphery of the catalytic core (2). CcO is embedded in the mitochondrial inner membrane (IM) and exists as supercomplexes with respiratory complex III in yeast and in complexes I and III in metazoans (3). The biogenesis of CcO commences with the mitochondrial synthesis of Cox1–Cox3 subunits followed by the insertion of heme and copper cofactors and the addition of the imported nuclear subunits synthesized in the cytoplasm.

A series of assembly factors facilitate Cox1 maturation and cofactor insertion. The process of CcO biogenesis is best defined in the yeast *Saccharomyces cerevisiae*. An IM-tethered translational activator Pet309 along with Mss51 stimulates *COX1* translation (4–7). IM insertion of Cox1 occurs in a co-translational manner with the Oxa1 translocase (8, 9). Mss51 has a second function in translational elongation of Cox1, and this occurs within a polyprotein complex consisting of Mss51, Cox14, Coa3, and Ssc1 (7, 10–13). Cox1 maturation involves progression from this Mss51-containing complex to downstream transient assembly complexes involving Coa1 and Shy1 (11, 14). Many CcO assembly mutants attenuate *COX1* translation through sequestration of Mss51 within the Mss51-containing Cox1 complex (10). The C-terminal tail of Cox1, not embedded within the IM, mediates the formation of the sequestered Mss51-Cox14-Coa3-Ssc1 complex (15). This conformer of Cox1 is shielded from rapid proteolysis and may serve as a Cox1 storage reservoir poised to initiate CcO biogenesis. Mss51 release from this Cox1-containing complex is dependent on either association of two nuclear subunits Cox5a and Cox6 or the insertion of Shy1 into the complex (7, 10–13). Formation of the heme and copper centers in Cox1 occurs upon release of Mss51-stalled complex and likely within the Shy1-containing complex (16). The two heme groups in CcO are modified hemes containing a hydroxyethylfarnesyl group and oxidized pyrrole methyl substituent. These heme modifications are catalyzed by the Cox10 farnesyl transferase and Cox15 heme oxidase (17).

Coa2 is another factor participating in Cox1 maturation. Cells lacking Coa2 are stalled in CcO biogenesis and exhibit a rapid degradation of newly synthesized Cox1 leading to impaired CcO biogenesis (18). Cox1 translation proceeds normally, as does formation of the Mss51-Cox14-Coa3-Ssc1 complex with newly synthesized Cox1. However, Cox1 maturation is impeded by its facile degradation. The respiratory deficiency of *coa2*Δ cells is suppressed by one of two mechanisms (19). First, a N196K mutant allele of the Cox10 farnesyl transferase was found to be a robust gain-of-function suppressor of the respiratory deficiency of *coa2*Δ cells (19). The mutant Cox10 enzyme exhibits an unusually stable oligomeric complex that correlates with an active enzymatic state in catalyzing the farnesylation of heme *b*. Cox10 activation appears to be the rate-limiting step in the hemylation process (20). Enhanced catalytic activity of the mutant Cox10 is likely responsible for reversing the attenuation in Cox1 hemylation in *coa2*Δ cells.

The second mechanism that restores respiratory function in *coa2*Δ cells is by the disruption of the Oma1 IM protease (19). Oma1 is one of several quality control proteinases within the

* This work was supported, in whole or in part, by National Institutes of Health, NIEHS Grant ES03817 (to D. R. W.). This work was also supported by American Heart Association Grant 10POST4300044 (to O. K.).

[1] To whom correspondence should be addressed: Dept. of Medicine, University of Utah Health Sciences Ctr., SOM 5C 426, Salt Lake City, UT 84132. Tel.: 801-585-5103; Fax: 801-585-3432; E-mail: dennis.winge@hsc.utah.edu.

[2] The abbreviations used are: CcO, cytochrome *c* oxidase; IM, inner membrane; BN-PAGE, blue-native PAGE; mAAA, inner membrane protease with matrix-facing catalytic center; iAAA, inner membrane protease with IMS-facing catalytic center.

TABLE 1
Yeast strains used in this work

Strain	Genotype	Ref.
W303	*MATα ade2-1 his3-1,15 leu2-3,112 trp1-1 ura3-1* [*rho*$^+$]	
DY5113	*MAT***a** *ade2-1 his3-1,15 leu2-3,112 trp1*Δ *ura3-1* [*rho*$^+$]	
*oma1*Δ	*MATα ade2-1 his3-1,15 leu2-3,112 trp1-1 ura3-1 oma1*Δ::*CaURA3* [*rho*$^+$]	Ref. 19
*coa2*Δ	*MATα ade2-1 his3-1,15 leu2-3,112 trp1-1 ura3-1 coa2*Δ::*KanMX4* [*rho*$^+$]	Ref. 18
*coa1*Δ	*MATα ade2-1 his3-1,15 leu2-3,112 trp1-1 ura3-1 coa1*Δ::*KanMX4* [*rho*$^+$]	Ref. 11
*cox4*Δ	*MATα ade2-1 his3-1,15 leu2-3,112 trp1-1 ura3-1 cox4*Δ::*URA3* [*rho*$^+$]	Ref. 17
*cox11*Δ	*MAT***a** *ade2-1 his3-1,15 leu2-3,112 trp1-1 ura3-1 cox11*Δ::*HIS3* [*rho*$^+$]	Ref. 24
*shy1*Δ	*MATα ade2-1 his3-1,15 leu2-3,112 trp1-1 ura3-1 cox11*Δ::*URA3* [*rho*$^+$]	Ref. 11
*cox14*Δ	*MATα ade2-1 his3-1,15 leu2-3,112 trp1-1 ura3-1 cox14*Δ::*HIS3* [*rho*$^+$]	Ref. 17
*qcr7*Δ	*MATα ade2-1 his3-1,15 leu2-3,112 trp1-1 ura3-1 qcr7*Δ::*TRP1* [*rho*$^+$]	B. Trumpower
*cox10*Δ	*MATα ade2-1 his3-1,15 leu2-3,112 trp1-1 ura3-1 cox10*Δ::*HIS3* [*rho*$^+$]	Ref. 17
*cox15*Δ	*MAT***a** *ade2-1 his3-1,15 leu2-3,112 trp1*Δ *ura3-1 cox15*Δ::*KanMX4* [*rho*$^+$]	This study
*coa2*Δ*oma1*Δ	*MATα ade2-1 his3-1,15 leu2-3,112 trp1-1 ura3-1 coa2*Δ::*KanMX4 oma1*Δ::*CaURA3* [*rho*$^+$]	Ref. 19
*cox11*Δ*oma1*Δ	*MATα ade2-1 his3-1,15 leu2-3,112 trp1-1 ura3-1 cox11*Δ::*HIS3 oma1*Δ::*CaURA3* [*rho*$^+$]	This study
*cox4*Δ*oma1*Δ	*MATα ade2-1 his3-1,15 leu2-3,112 trp1-1 ura3-1 cox4*Δ::*URA3 oma1*Δ::*HIS3MX6* [*rho*$^+$]	This study
*cox14*Δ*oma1*Δ	*MAT***a** *ade2-1 his3-1,15 leu2-3,112 trp1*Δ *ura3-1 cox14*Δ::*KanMX4 oma1*Δ::*HIS3MX6* [*rho*$^+$]	This study
*qcr7*Δ*oma1*Δ	*MATα ade2-1 his3-1,15 leu2-3,112 trp1-1 ura3-1 qcr7*Δ::*TRP1 oma1*Δ::*HIS3MX6* [*rho*$^+$]	This study
*yme1*Δ*oma1*Δ	*MATα ade2-1 his3-1,15 leu2-3,112 trp1-1 ura3-1 yme1*Δ::*HIS3MX6 oma1*Δ::*CaURA3* [*rho*$^+$]	This study
*coa2*Δ*cox10*Δ	*MATα ade2-1 his3-1,15 leu2-3,112 trp1-1 ura3-1 coa2*Δ::*CaURA3 cox10*Δ::*HIS3* [*rho*$^+$]	This study
*coa2*Δ*cox15*Δ	*MATα ade2-1 his3-1,15 leu2-3,112 trp1-1 ura3-1 coa2*Δ::*KanMX4 cox15*Δ::*CaURA3* [*rho*$^+$]	Ref. 19
*cox11*Δ*cox10*Δ	*MAT***a** *ade2-1 his3-1,15 leu2-3,112 trp1-1 ura3-1 cox11*Δ::*HIS3 cox10*Δ::*CaURA3* [*rho*$^+$]	This study
*cox11*Δ*coa2*Δ	*MATα ade2-1 his3-1,15 leu2-3,112 trp1-1 ura3-1 cox11*Δ::*CaURA coa2*Δ::*HIS3MX6* [*rho*$^+$]	This study
*coa2*Δ*oma1*Δ*yta10*Δ	*MATα ade2-1 his3-1,15 leu2-3,112 trp1-1 ura3-1 coa2* Δ::*KanMX4 oma1*Δ::*TRP1 yta10*Δ::*HIS3MX6* [*rho*$^+$]	This study
SHY1-13Myc	*MAT***a** *ade2-1 his3-1,15 leu2-3,112 trp1*Δ *ura3-1 SHY1*-13Myc::*TRP1* [*rho*$^+$]	Ref. 11
OMA1-13Myc	*MAT***a** *ade2-1 his3-1,15 leu2-3,112 trp1*Δ *ura3-1 OMA1*-13Myc::*HIS3MX6* [*rho*$^+$]	This study
OMA1-13Myc *coa2*Δ	*MAT***a** *ade2-1 his3-1,15 leu2-3,112 trp1*Δ *ura3-1 OMA1*-13Myc::*HIS3MX6 coa2*Δ::*KanMX4* [*rho*$^+$]	This study
OMA1-13Myc *cox11*Δ	*MAT***a** *ade2-1 his3-1,15 leu2-3,112 trp1*Δ *ura3-1 OMA1*-13Myc::*HIS3MX6 cox11*Δ::*CaURA3*[*rho*$^+$]	This study
YMN503	*MAT***a** *ade2-1 his3-1,15 leu2-3,112 trp1-1 ura3-1 yta10* Δ::*KanMX4 mrpl32*Δ::*NatMX4* (p*Su9-MRPL32*) [*rho*$^+$]	Ref. 32
YMN503 *coa2*Δ	*MAT***a** *ade2-1 his3-1,15 leu2-3,112 trp1-1 ura3-1 yta10* Δ::*KanMX4 mrpl32*Δ::*NatMX4* (p*Su9-MRPL32*) *coa2*Δ::*HphMX4* [*rho*$^+$]	This study
YMN503 *oma1*Δ	*MAT***a** *ade2-1 his3-1,15 leu2-3,112 trp1-1 ura3-1 yta10* Δ::*KanMX4 mrpl32*Δ::*NatMX4* (p*Su9-MRPL32*) *oma1*Δ::*TRP1* [*rho*$^+$]	This study
XPM209	*MATα lys2*Δ *arg8*Δ::*hisG ura3-52 leu2-3,112* [*COX1*Δ *C15 rho*$^+$]	Ref. 15
YC65	*MATα lys2*Δ *arg8*Δ::*hisG ura3-52 leu2-3,112 cox11*Δ::*KanMX4* [*COX1*Δ *C15 rho*$^+$]	Ref. 15
XPM209 *coa2*Δ	*MATα lys2*Δ *arg8*Δ::*hisG ura3-52 leu2-3,112 coa2*Δ::*CaURA3* [*COX1*Δ *C15 rho*$^+$]	This study
XPM209 *oma1*Δ	*MATα lys2*Δ *arg8*Δ::*hisG ura3-52 leu2-3,112 oma1*Δ::*CaURA3* [*COX1*Δ *C15 rho*$^+$]	This study
XPM209 *coa2*Δ*oma1*Δ	*MATα lys2*Δ *arg8*Δ::*hisG ura3-52 leu2-3,112 coa2*Δ::*CaURA3 oma1*Δ::*KanMX4* [*COX1*Δ *C15 rho*$^+$]	This study
XPM209 *cox11*Δ*oma1*Δ	*MATα lys2*Δ *arg8*Δ::*hisG ura3-52 leu2-3,112 cox11*Δ::*KanMX4 oma1*Δ::*CaURA3* [*COX1*Δ *C15 rho*$^+$]	This study

mitochondria. Unlike two major quality control proteases in the IM, mAAA and iAAA, Oma1 contains only a metalloproteinase domain and lacks the ATPase function involved in extrusion of proteins from the membrane bilayer. The restoration of respiratory capacity in *coa2*Δ cells by elimination of Oma1 may occur by allowing more time for the inefficient Cox1 hemylation process. A similar situation has been recently described in which impairment in ER proteolysis rescues the activity of unstable lysosomal proteins by prolonging ER retention (21).

In the present study, we address the substrate specificity of Oma1 in the degradation of mitochondrially synthesized component of CcO and the bc_1 complex. We show presently that Oma1 protease mediates Cox1 degradation in *coa2*Δ cells but not other cells stalled in CcO biogenesis. The facile degradation of Cox1 in *coa2*Δ cells arises not merely from Oma1 activation in the mutant but likely from the misfolded Cox1 conformer that is an efficient substrate for Oma1-mediated proteolysis.

EXPERIMENTAL PROCEDURES

Strains and Growth Media—S. cerevisiae strains used in this study are listed in Table 1. Yeast cells were grown in YP (1% yeast extract, 2% bactopeptone) or SC minimal medium, supplemented with respective amino acids. The carbon source used was either 1 or 2% glucose, 2% galactose, or glycerol/lactate. The chromosomal loci of the respective genes in yeast cells were either tagged with a 13xMyc epitope tag at the 3′ position or disrupted by homologous recombination as described previously (11). Each disruption or gene modification was confirmed by PCR analyses of the respective locus. *Escherichia coli* DH5α cells, used for cloning and plasmid propagation, were cultured and handled as described previously (22).

Vectors and Constructs—Standard procedures were used for all manipulations with DNA fragments and plasmids (22). YEp352-*MSS51*, pRS423-*MSS51*, pRS426-*SSC1*, YEp352-*MDJ1* (11), and pRS425-*COA2* (18) plasmids were used in this study. All constructs were verified by sequencing. Plasmids were transformed into the yeast cells using lithium acetate procedure (23).

Hydrogen Peroxide Sensitivity, Respiratory Growth, and Mitochondrial Reactive Oxygen Species Quantification Assays—Sensitivities of the yeast strains and transformants to hydrogen peroxide were tested as described previously (24). For a large-scale treatment of the cultures with H_2O_2, the cells were grown overnight at 30 °C in 1 liter of YP with 2% glucose to A_{600} of 2.0–3.0, diluted with the fresh medium to optical density of 1.0–1.5 and cultivated for 2 h with or without 6 mM H_2O_2 added. Followed the incubation, cells were harvested, and their mitochondria were isolated as described below. To test the respiratory competence, strains were grown overnight in selective medium containing 2% glucose, serially diluted, and spotted on glucose-containing medium (control) and 2% glycerol/2% lactate-containing rich or synthetic medium.

The levels of the reactive oxygen species generated by various yeast strains were quantified using the superoxide-sensitive fluorescent dye MitoSox (Invitrogen). Unsynchronized cultures were grown for 24 or for 48 h in the liquid YP medium with 2% glucose. An aliquot of each respective culture (5×10^6 ml^{-1} cells) was washed twice in PBS buffer (137 mM NaCl, 2.7 mM

KCl, 10 mM Na_2HPO_4, 2 mM K_2HPO_4, pH 7.4) and incubated with or without 5 μM MitoSox for 10 min at 37 °C in the dark. Followed the incubation, samples were washed three times with PBS buffer and subjected to mild sonication for 1 min to disperse aggregated cells. FACS analysis of the stained samples was carried using FACscan flow cytometer (Becton Dickinson). MitoSox fluorescence was measured in FL-2H channel. FCS Express 3.0 program (DeNovo Software) was used for data analysis. Cell viability was assessed using cell staining with 1 μM Cytox Green fluorescent dye (Invitrogen) according to the manufacturer's instructions.

Mitochondria Isolation and Assays—Intact mitochondria were isolated from yeast cells as described (25). Mitochondrial protein concentrations were quantified by the Bradford assay (26). Specific CcO, aconitase, and succinate dehydrogenase enzymatic activities were determined as described (27–29). The specific activities were normalized to mitochondrial protein levels and presented as a percentage of wild-type activity. Separation of the intact mitochondrial protein complexes by blue-native PAGE (BN-PAGE) was performed as described previously (16). Complexes were resolved on a continuous 5–13% gradient gel, transferred onto a PVDF membrane, and analyzed by Western blot. For second-dimension SDS-PAGE analysis, lanes were cut out, incubated in 1% SDS-1% β-mercaptoethanol for 1 h at 25 °C, run on a 12% denaturing SDS-PAGE gel, and assessed by immunoblotting. Fractionation of the mitochondrial complexes in the continuous 7–30% sucrose gradients by high-velocity centrifugation was conducted as described previously (16).

Assessment of Proteolytic Activity—Proteolytic activity in the mitochondrial membranes was measured following the method adapted from Bulteau *et al.* (30). Mitochondria isolated from various strains were resuspended in hypotonic buffer (20 mM HEPES, pH 7.4) and gently sonicated (3 × 30 s with 50% duty cycle). Obtained mixtures were fractionated at 165,000 × *g* for 1 h at 2 °C, and pellet fractions were collected for further analysis. Reisolated mitochondrial membranes (25 μg) were preincubated in 150 μl of the reaction buffer (10 mM $MgCl_2$, 1.0 mM DTT, 0.05% Triton X-100, 50 mM Tris-HCl, pH 7.9) with or without 8 mM ATP for 5 min at 25 °C. The reaction was then started by adding 5 μM (final concentration) FITC-casein (Sigma) to each sample. The samples were allowed to incubate at 25 °C for 35 min in the dark. Followed the incubation, 100 μl of 50 mM Tris-HCl (pH 7.9) buffer were added and unhydrolyzed FITC-casein, and the membranes were removed by centrifugation at 20,000 × *g* for 20 min at 4 °C. The TCA precipitation step was omitted to increase the sensitivity of the method. Next, 250 μl of each supernatant containing the peptide fragments were mixed with 200 μl of 50 mM Tris-HCl, pH 7.9. Samples were further diluted 10-fold with double-distilled water to avoid the light scattering. The fluorescence intensities were determined using an excitation wavelength of 445 nm and an emission wavelength of 515 nm in a PerkinElmer LS55 Fluorescence Spectrometer. Obtained values were normalized to fluorescence of the same amount of FITC-casein incubated without mitochondrial membranes.

In Vivo Labeling of Mitochondrial Translation Products—Yeast cells precultured overnight in either complete or supplemented SC medium containing 2% raffinose or galactose, reinoculated and grown to an A_{600} of 0.8. The labeling, preparation, and separation of the samples by SDS-PAGE were done as described (31). Gels were dried, and separated radiolabeled proteins were visualized by autoradiography. Intensities of the bands were quantified using NIH ImageJ software (http://rsb.info.nih.gov/ij/).

Preparation of Yeast Whole-cell Extracts—Whole-cell extracts were prepared from the cells grown at 30 °C in 50 ml of YP with 2% glucose or raffinose to A_{600} of 1.0–4.0. Cells were harvested by centrifugation at 20,000 × *g* for 5 min at RT, washed with distilled water and pelleted again. Collected cell pellets were resuspended in 250 μl of 50 mM Tris-HCl, pH 8.0, and mixed with 50 μl of lysis buffer (10 M NaOH, 7.5% β-mercaptoethanol, 2 mM phenylmethylsulfonyl fluoride). Following the 10-min incubation on ice, cold TCA was added to a final concentration of 25%. Samples were vigorously mixed, kept on ice for 15 min, and centrifuged (15 min at 20,000 × *g* at 4 °C). Pellets were washed with 80% cold acetone, spun down for 10 min (20,000 × *g* at 4 °C), resuspended in 1× SDS-Laemmli buffer, and incubated at 56 °C for 15 min. A fraction of the each respective sample was subjected to SDS-PAGE followed by immunoblot analysis.

Immunoassays—For immunoblot analysis, mitochondrial or total TCA-precipitated proteins were loaded onto a denaturing 12% polyacrylamide gel, subjected to SDS-PAGE, and transferred onto a nitrocellulose or PVDF membrane. Transferred polypeptides were detected with indicated primary antibodies and visualized with either ECL reagents (Pierce) or the Odyssey Infrared Imaging System (LI-COR Biosciences), respectively, when horseradish peroxidase-conjugated or fluorescent secondary antibodies were used. Anti-Myc antibody was obtained from Roche Diagnostic. Antibodies to the mitochondrial outer membrane porin were from Invitrogen. Dr. Alex Tzagoloff kindly provided Atp2 (F_1) antiserum.

RESULTS

Oma1 and Not mAAA Mediates Cox1 Degradation in coa2Δ Cells—One dramatic phenotype of *coa2*Δ cells is the facile degradation of Cox1 (11). Cox1 is synthesized efficiently, and the initial Mss51-containing assembly intermediate forms normally; however, Cox1 is degraded rapidly. We reported previously that respiratory activity was restored in *coa2*Δ cells by the elimination of the Oma1 metalloproteinase (19). The disruption of the ATP-dependent protease iAAA showed no effect, whereas the disruption of the mAAA with a hypomorphic mAAA mutant had a modest effect (18). Because the mAAA protease is known to mediate degradation of membrane proteins, we initially reassessed the role of mAAA in Cox1 degradation. The mAAA protease consists of hetero-oligomeric complex containing Yta10 and Yta12. Protease activity is abolished by the deletion of either *YTA10* or *YTA12*. Such mutants are impaired in the processing of the MrpL32 subunit of the mitoribosome and therefore exhibit an unstable mitochondrial genome (32). Respiratory function is restored by the expression of a MrpL32 variant that does not require mAAA processing (32). To reinvestigate the role of mAAA in Cox1 degradation in *coa2*Δ cells, we constructed a mutant lacking Coa2 and mAAA function

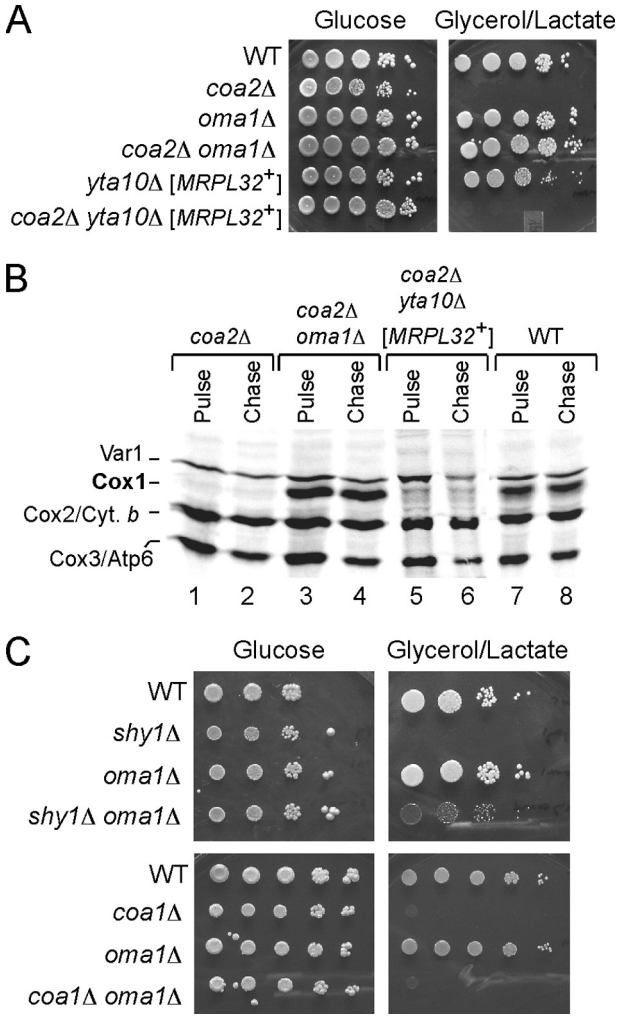

FIGURE 1. **Oma1 specifically mediates Cox1 degradation in *coa2*Δ cells.** *A*, respiratory growth of Coa2-deficient cells lacking various proteases. Cells were pregrown in complete liquid medium, serially diluted, and spotted onto plates containing 2% glucose or glycerol/lactate as a carbon source. *B*, *in vivo* labeling of mitochondrial translation products in the cells described in *A*. The cells were pulsed for 15 min with [^{35}S]methionine at 30 °C. The reaction was stopped by addition of cold methionine. Following a 60-min chase at 30 °C, samples were subjected to 12% SDS-PAGE and analyzed by autoradiography. *C*, respiratory growth of the *shy1*Δ and *coa1*Δ strains with and without Oma1. Cells were handled as described in *A*. *Cyt. b*, cytochrome *b*.

(*yta10*Δ with the heterologous *MRPL32*). The elimination of all mAAA protease activity in *coa2*Δ cells did not restore any respiratory growth unlike the elimination of Oma1 (Fig. 1*A*). However, the addition of WT Coa2 to the *coa2*Δ*yta10*Δ mutant cells restored respiratory growth ruling out respiratory deficiency arising from loss of the mitochondrial genome (data not shown). We also tested whether the loss of mAAA activity restored levels of newly synthesized Cox1 using a mitochondrial protein translation assay in which cells were labeled with [^{35}S]methionine in the presence of cycloheximide to block translation in the cytoplasm. Only mitochondrial translation products, including Cox1, are labeled in this protocol. Whereas the loss of Oma1 in *coa2*Δ cells restored newly synthesized Cox1, no appreciable restoration was apparent with the loss of mAAA function (Fig. 1*B*). These data confirm that Oma1 plays a major role in Cox1 degradation in *coa2*Δ cells.

*Oma1-mediated Cox1 Degradation Is Restricted to coa2*Δ *Cells*—Coa1 and Shy1 are two other CcO assembly factors that function in maturation of newly synthesized Cox1. Genetic analyses suggest these factors function in conjunction with Coa2. Cells lacking either Coa1 or Shy1 in certain *S. cerevisiae* genetic backgrounds exhibit a CcO deficiency and assembly intermediates are degraded. To assess whether Oma1 mediates the degradation of Cox1 in these mutant backgrounds, *OMA1* was deleted in either *coa1*Δ or *shy1*Δ cells (Fig. 1*C*). The elimination of Oma1 from *shy1*Δ cells gave a very modest improvement in respiratory growth, but not with *coa1*Δ cells. Thus, the removal of Oma1 in *coa2*Δ cells is unique in yielding a dramatic improvement in respiratory function.

To address whether Oma1 is a general Cox1 quality control protease, we addressed the turnover of Cox1 in three mutants stalled in CcO biogenesis, namely *cox14*Δ, *cox11*Δ, and *cox4*Δ cells. These mutants stall Cox1 maturation at early to late steps, respectively. To monitor newly synthesized Cox1, we used the mitochondrial translation assay mentioned above. It should be pointed out that Cox1 translation is attenuated markedly in most CcO assembly mutants due to sequestration of Mss51 (10). This attenuation in Cox1 synthesis is apparent in *cox11*Δ and *cox4*Δ cells but pulse chase studies reveal that the newly synthesized Cox1 is still labile, relative to the pulse levels (Fig. 2*A*). Cox1 is equally labile in *cox11*Δ cells regardless of the presence or absence of Oma1 (Fig. 2*A*). The turnover of Cox1 in *cox4*Δ cells is likewise unaffected by the presence or absence of Oma1 (Fig. 2*A*). Cells lacking Cox14 do not exhibit the same attenuation in Cox1 synthesis (10). However, newly synthesized Cox1 is unstable in *cox14*Δ cells (12). The deletion of *OMA1* in these cells does not alter the rate of Cox1 turnover (Fig. 2*A*).

It is difficult to compare Cox1 degradation rates in various CcO assembly mutants because Cox1 synthesis is attenuated in many but not all mutants due to sequestration of Mss51 (10). Therefore, we took advantage of the recently described genetic system involving the deletion of the C-terminal 15 residues in Cox1 (15). The C-terminal residues of Cox1 are important for the Mss51/Cox14 binding that is required for Mss51 sequestration (15). Although Cox1 synthesis proceeds normally, Cox1ΔC15 is partially labile and the cells are impaired in respiratory growth at elevated temperatures (data not shown). Cells containing the Cox1ΔC15 truncate were compared in the mitochondrial translation assay to deletion strains engineered in this background that lack either Cox11 or Coa2 (Fig. 3*A*). In the absence of Mss51 sequestration, the Cox1 synthesis rate is comparable in various mutants (Fig. 3*A*, *lane 1*), thereby allowing comparisons in turnover rates. The turnover of Cox1 is enhanced in *coa2*Δ cells relative to *cox11*Δ cells (Fig. 3*B*), highlighting the facile Cox1 degradation process in *coa2*Δ cells. To evaluate the role of Oma1 in Cox1 degradation in these strains, *OMA1* was deleted in both *coa2*Δ and *cox11*Δ cells containing the C-terminal truncated Cox1. The elimination of Oma1 in *coa2*Δ cells stabilizes Cox1 during the chase (Fig. 3, *bottom panel*), whereas no appreciable change in Cox1 degradation occurred in *cox11*Δ cells upon loss of Oma1.

We evaluated whether Oma1 contributed to the degradation of an IM protein distinct from Cox1. We focused on the mitochondrial encoded cytochrome *b* subunit of the bc_1 complex.

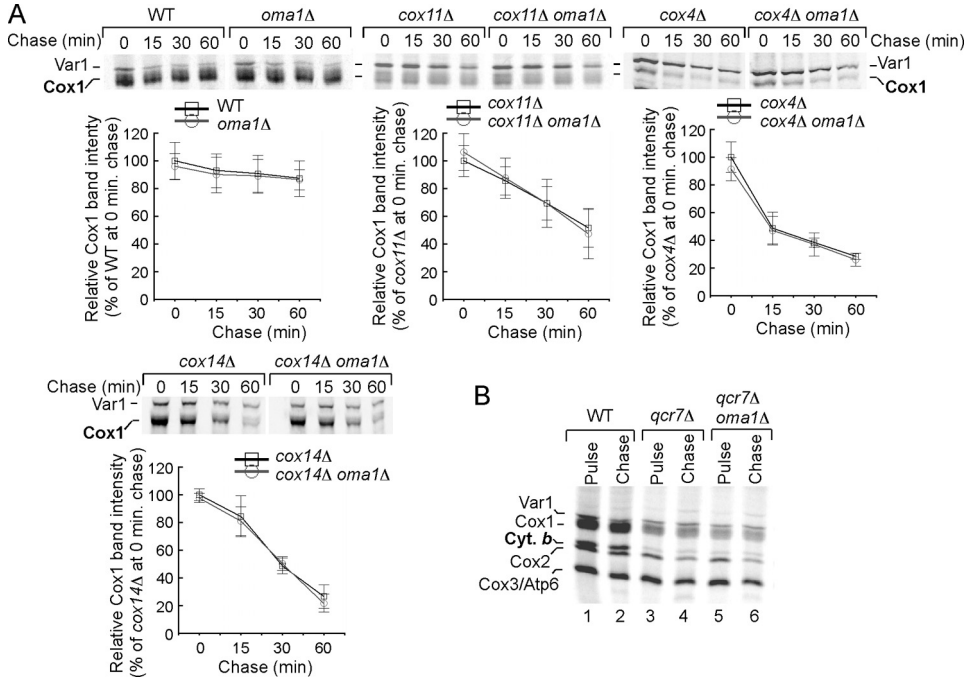

FIGURE 2. **Cox1 degradation in CcO assembly mutants with and without Oma1.** *A*, degradation kinetics of the newly synthesized Cox1 in wild-type, *cox11*Δ, *cox4*Δ, and *cox14*Δ strains with and without Oma1. Cells were pulsed with [^{35}S]methionine as described in Fig. 1*B*. Aliquots were taken at indicated chase time points, and Cox1 degradation was assessed as a percentage of the signal abundance in each respective band. The intensities of Cox1 bands were normalized to the ones of the respective Var1 and cytochrome *b* (*Cyt. b*) signals. The data represent an average of three independent experiments; the *error bars* indicate S.D. *B*, *in vivo* labeling of mitochondrial translation products in the WT, *qcr7*Δ and *qcr7*Δ*oma1*Δ cells. *Cyt. b*, cytochrome *b*.

Cells lacking Qcr7 stall maturation of the bc_1 complex leading to rapid cytochrome *b* degradation (33). To address whether Oma1 contributes to the degradation cytochrome *b*, we compared *qcr7*Δ cells to *qcr7*Δ *oma1*Δ double null cells (Fig. 2*B*). The turnover of cytochrome *b* was unaffected by the presence or absence of Oma1. Thus, Oma1 exhibits selective proteolysis of Cox1 in *coa2*Δ cells.

*Oma1-dependent Proteolysis Is Enhanced in coa2*Δ *Cell Mitochondria*—The observed proteolysis of Cox1 in *coa2*Δ cells implies that Oma1 is active in the mutant cells. To test whether Oma1 activation occurs in such cells, we took advantage of two proteolysis assays. First, we isolated mitochondrial membranes from respective cells and monitored the proteolysis of FITC-casein. Casein is an efficient substrate for many proteases due to its non-compact structure. Mitochondrial membranes derived from *coa2*Δ cells showed a significant elevation in FITC-casein proteolysis, whereas it was attenuated in membranes isolated from *coa2*Δ*oma1*Δ cells (Fig. 4*A*). The assay was conducted in the presence or absence of ATP. Two major membrane proteases are the ATP-dependent mAAA and iAAA enzymes. AAA proteases are largely inactive without the addition of ATP (34). In the absence of ATP, the effect of Oma1 on FITC-casein is readily apparent. The level of FITC-casein proteolysis in the double mutant was equivalent to the level with membranes isolated from wild-type cells. The second proteolysis assay involved the pre-isolation of the ~450 kDa Cox1-containing Shy1 complex from wild-type cells (Fig. 4*B*). The high mass Shy1 complex containing Cox1 was recovered from sucrose gradient ultracentrifugation. BN-PAGE was used to document the presence of the complex. Previous data revealed that the heme *a* and Cu_B cofactors sites are likely populated within this intermediate (16). To address Oma1 proteolysis using the Shy1 complex as a substrate, the Shy1 complex was incubated with membrane fractions described in Fig. 4*A* for 35 min followed by BN-PAGE analysis and visualization of Myc-tagged Shy1 by immunoblotting (Fig. 4*C*). Membranes isolated from WT cells lacking an epitope-tagged Shy1 did not perturb the abundance of the Shy1-Myc complex, whereas incubation with membranes isolated from *coa2*Δ cells led to the loss of the complex. Although the complex is depleted, the Shy1 protein itself remains intact. The addition of membranes isolated either from *oma1*Δ or *coa2*Δ *oma1*Δ cells did not lead to the same loss of the Shy1 complex seen in *coa2*Δ cells. These two assays suggest that Oma1-mediated proteolysis is activated in *coa2*Δ cells and contributes to the Cox1 degradation or disassembly of the Cox1 assembly intermediate.

*Oligomeric Oma1 Complex Altered in coa2*Δ *Cells*—The facile Oma1-mediated degradation of Cox1 seen in *coa2*Δ cells suggests that a specific condition exists within the mutant cells leading to the degradation. This condition may activate Oma1 or result in a Cox1 conformer that is highly susceptible to degradation. We initially focused on the state of Oma1 in *coa2*Δ cells. In these studies *OMA1* was chromosomally tagged with a C-terminal Myc epitope. The disruption of *COA2* in these cells led to the same rapid Cox1 degradation suggesting the chimeric protein is functional (data not shown). The abundance and size of Oma1 was unperturbed comparing WT to *coa2*Δ cells on steady-state SDS-PAGE (Fig. 5*A*). Oma1 exists within a high mass complex that was postulated to be a homo-oligomeric species (35). The abundance of this complex observed on BN-PAGE is attenuated in *coa2*Δ cells (Fig. 5*B*). Steady-state levels

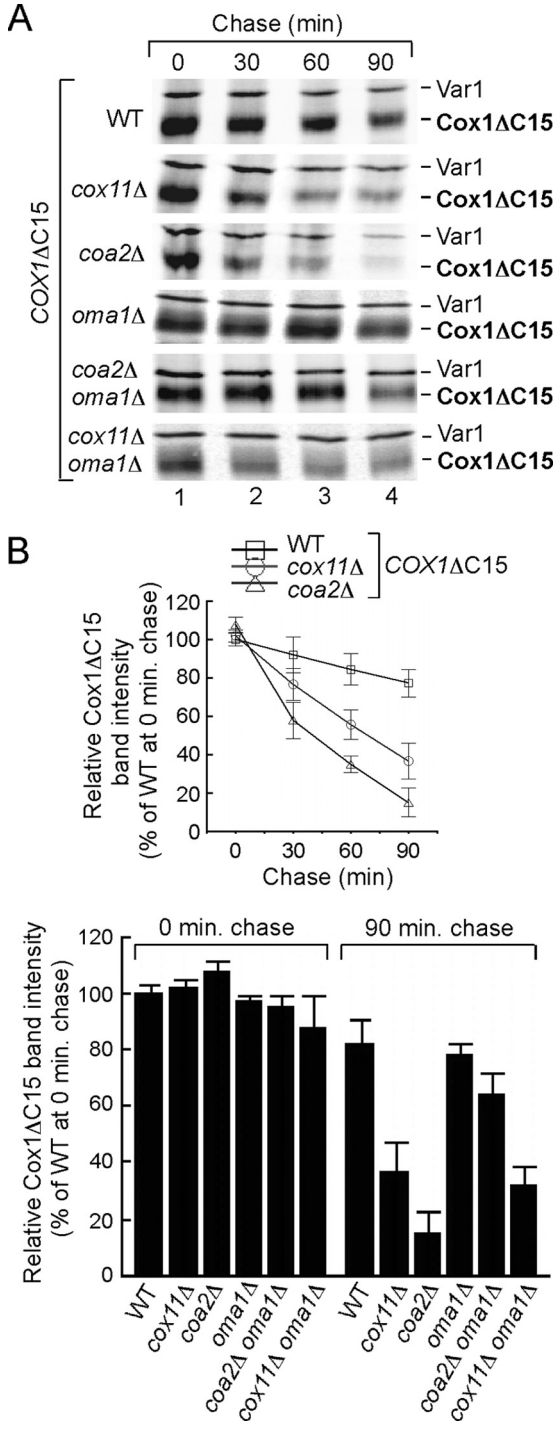

FIGURE 3. **Cox1ΔC15 degradation in CcO assembly mutants with and without Oma1.** Shown are representative chase autoradiograms (*A*) and degradation kinetics (*B*) of Cox1ΔC15 in WT, *cox11*Δ, *coa2*Δ, *oma1*Δ, *coa2*Δ*oma1*Δ, and *cox11*Δ*oma1*Δ cells. Lack of the 15 C-terminal residues in Cox1 relieves its translational attenuation in the respective mutants; however, the degradation rates of Cox1ΔC15 differ between *cox11*Δ and *coa2*Δ mitochondria. Intensities of Cox1ΔC15 were assessed as described in Fig. 2; *error bars* indicate S.D. ($n = 3$).

and the size of Oma1, as assessed by SDS-PAGE, were not altered in *coa2*Δ cells. Thus, neither the expression nor any proteolytic processing of Oma1 was apparent in *coa2*Δ cells. To assess why Oma1 was not visible on BN-PAGE of mitochondria of the mutant cells, we conducted a two dimensional BN-PAGE experiment to assess whether the epitope was less accessible. Separation of proteins in the second dimension by SDS-PAGE resulted in the appearance of Oma1 at a lower apparent mass on the native PAGE dimension in *coa2*Δ cells (Fig. 5*C*).

As we reported previously, *coa2*Δ cells exhibit limited sensitivity to hydrogen peroxide (18). To assess whether oxidative stress conditions may contribute to the change in Oma1, we tested WT cells treated with hydrogen peroxide. A similar perturbation in Oma1 was apparent in the treated WT cells (Fig. 5, *D–F*). Oma1 was not detected by single dimension BN-PAGE in peroxide-treated WT cells, but visible at a lower mass by two-dimensional PAGE. The same is true with chronically hyperpolarized mitochondria (data not shown). Steady-state levels of Oma1 and its size were also not altered by the peroxide treatment (Fig. 5*E*). Thus, the physical state of the Oma1 complex is altered in *coa2*Δ and stressed WT cells. Dual affinity purification of Oma1 from WT cells was carried out to ascertain if other proteins existed in the high mass complex, but Oma1 was the only major protein detected by mass spectrometry analyses.

*Cox1 Degradation in coa2*Δ *Cells Is Not Primarily Related to Oxidative Stress*—The peroxide sensitivity of *coa2*Δ cells is abrogated by the deletion of *COX10* or *COX15* suggesting this sensitivity arises from the very low levels of pro-oxidant heme a_3:Cox1 (Fig. 6*A*) (24). Because Oma1 exhibited a conversion to a lower mass complex in both *coa2*Δ cells and peroxide-treated WT cells, we addressed whether the Cox1 degradation in *coa2*Δ cells was due to oxidant-triggered activation of Oma1. We initially screened *coa2*Δ cells for additional markers of oxidative stress. Cells lacking Coa2 exhibited reduced levels of aconitase but not succinate dehydrogenase activity (Fig. 6*B*). Aconitase, unlike succinate dehydrogenase, is highly susceptible to oxidative stress conditions due to the solvent-exposed iron atom in the iron-sulfur cluster (36). Another biomarker of oxidative stress is the mitochondrial MitoSox fluorophore that reports on levels of superoxide anion (37). Cells lacking Coa2 showed a marked elevation in MitoSox fluorescence by FACS analyses (Fig. 6*C*); this fluorescence is attenuated in *coa2*Δ cells lacking Cox10. The elimination of Cox10 in *coa2*Δ cells also partially reduces Oma1 proteolysis based on the FITC-casein assay, although the proteolytic activity is not returned to levels seen with WT membranes (Fig. 6*D*). The high mass Oma1 complex remains modified and cannot be observed by one dimensional BN-PAGE in *coa2*Δ*cox10*Δ cells (data not shown). These studies suggest that Oma1 may be activated in *coa2*Δ cells primarily due to the mitochondrial dysfunction of the mutant cells rather than oxidative stress.

An independent test of whether stress activation of Oma1 is responsible for Cox1 degradation in *coa2*Δ cells was conducted. We investigated the state of Oma1 in *cox11*Δ cells that are CcO-deficient and also are stressed oxidatively (24). Cox11 is a co-metallochaperone that mediates the copper metallation of the Cu_B site in Cox1 (38). Cells lacking Cox11 are sensitive to hydrogen peroxide due to the presence of the pro-oxidant heme a_3:Cox1 (24). The hydrogen peroxide sensitivity of *cox11*Δ cells is mitigated by the elimination of Cox10 (Fig. 7*A*). Cells lacking both Cox11 and Coa2 exhibit a peroxide sensitivity equivalent to the least sensitive of the two individual nulls, *coa2*Δ cells (Fig. 7*B*). In addition, *cox11*Δ cells exhibit elevated levels of super-

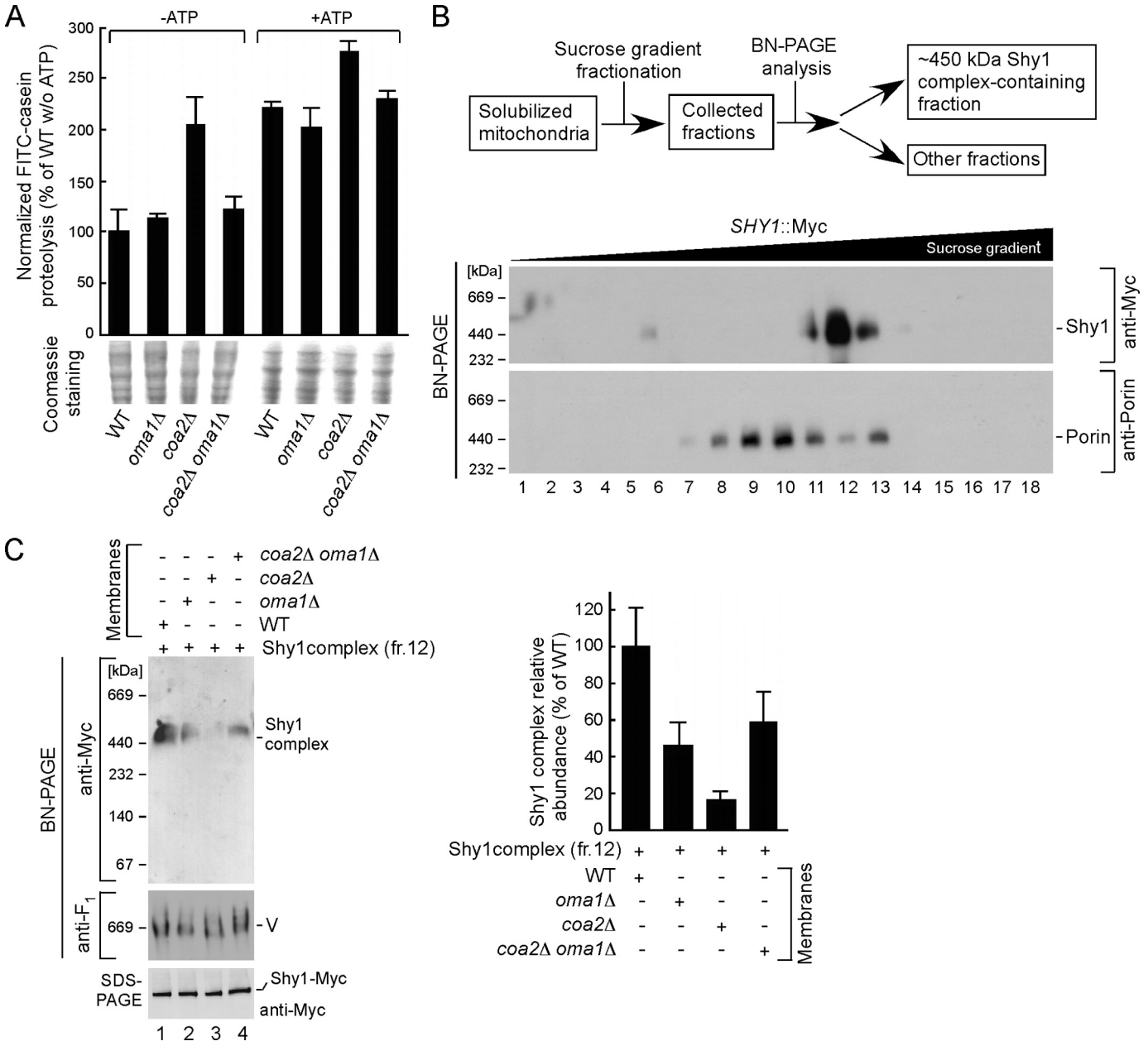

FIGURE 4. **Proteolytic activity of the mitochondrial membranes derived from *coa2*Δ cells.** *A*, *upper panel*: proteolytic activities of mitochondrial membranes. Organelles isolated from indicated strains were disintegrated and fractionated. Mitochondrial membrane fractions were collected and preincubated in the reaction buffer with (+) or without (−) 8 mM ATP. The assays were initiated by addition of FITC-casein, followed by incubation at 25 °C for 35 min. Reactions were stopped by rapid cooling of the samples, and the membranes as well as unhydrolized substrate were removed by high speed centrifugation. Supernatants were diluted 10-fold, and the fluorescence intensity was measured at excitation wavelength of 445 nm and an emission wavelength of 515 nm. The intensities were normalized to the fluorescence of FITC-casein incubated without membranes. The data represent an average of three independent repeats; the *error bars* indicate S.D. *Bottom panel*: the same amount of isolated membrane fractions (25 μg) subjected to SDS-PAGE and visualized by Coomassie staining served as loading control for proteolytic reaction. *B*, *upper panel*: schematic description of the ~450-kDa Shy1 complex isolation procedure. *Lower panel*, mitochondria (1.0 mg) from yeast strains expressing *SHY1*-Myc were lysed with 1% digitonin and clarified lysates loaded onto continuous 7–30% sucrose gradient and separated by the ultracentrifugation. Fractions were collected, and the distribution of ~450 kDa Shy1 and 440-kDa Porin complexes was analyzed by BN-PAGE and immunoblotting. *C*, the respective mitochondrial membranes (25 μg) were lysed in 1% digitonin, and clarified lysates have been incubated with an aliquot (15 μl) of the isolated fraction 12 (*fr. 12*) containing a ~450-kDa Shy1 complex. The mixtures were incubated as described in Fig. 3*A*. Following the 35-min incubation at 25 °C, samples were analyzed by either native or denaturing electrophoresis and immunoblotted with anti-Myc antibodies. Anti-F_1 serum was used to visualize the monomeric form of complex V (*V*), which served as a loading control for BN-PAGE. Intensities of the Shy1 complex were assessed as described in the legend to Fig. 2.

oxide anion as monitored by MitoSox fluorescence in FACS analyses (Fig. 7*B*). Overexpression of Oma1 failed to reverse the peroxide sensitivity of *cox11*Δ cells (Fig. 7*C*), suggesting the newly synthesized Cox1 in *cox11*Δ cells is more protected from degradation than in *coa2*Δ cells.

Oma1 is also converted in *cox11*Δ cells to a conformer that is not detected by single dimension BN-PAGE (Fig. 7*D*) but is seen at the lower mass position after two-dimensional gel electrophoresis (data not shown). Steady-state levels of Oma1 are not altered in *cox11*Δ cells. Because a correlation exists between Oma1

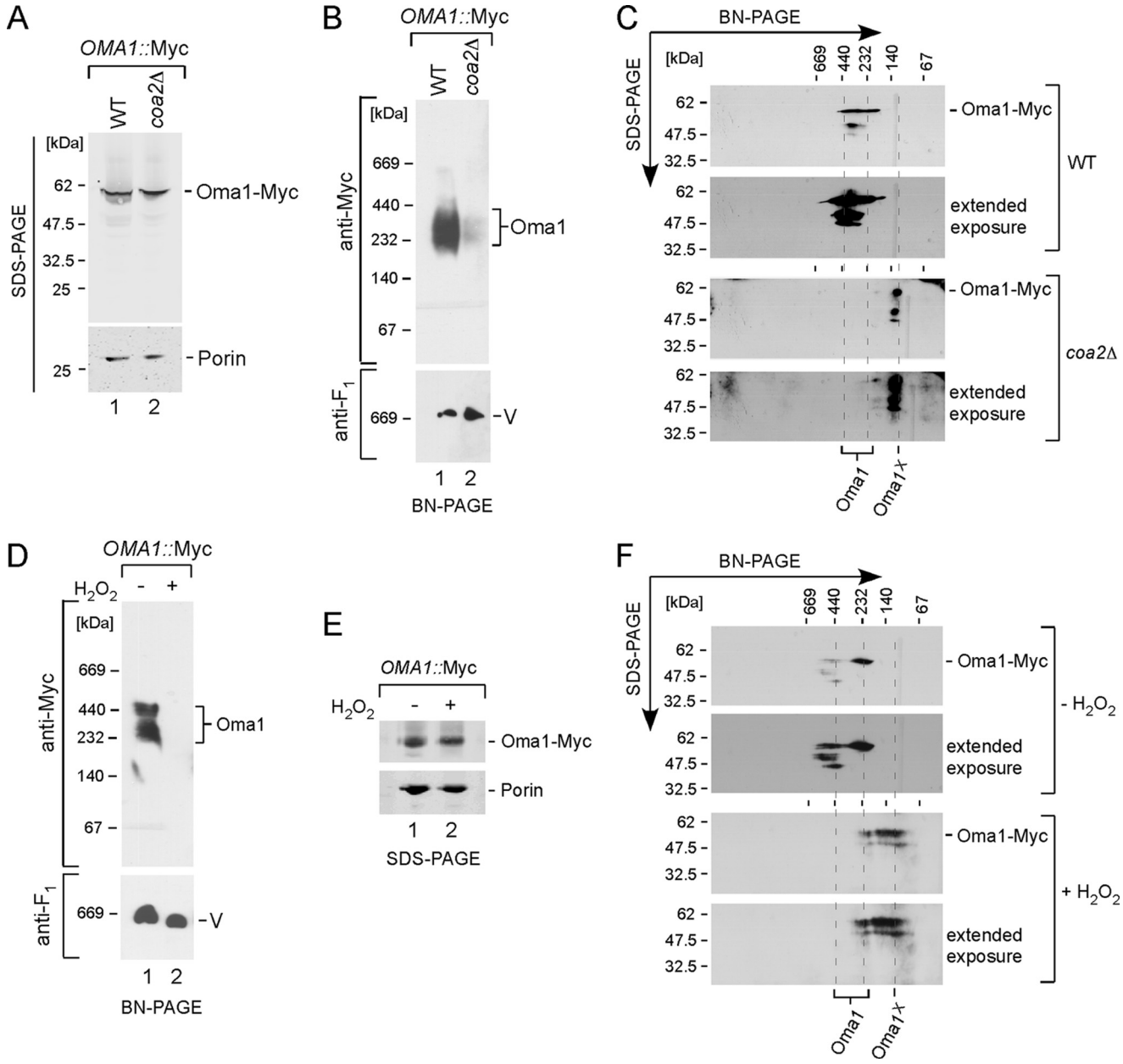

FIGURE 5. **Oma1 forms high molecular weight complex that is modified in *coa2*Δ cells and under stress conditions.** *A*, steady-state levels of Oma1 and porin in the *OMA1*::13Myc WT and *coa2*Δ strains. The TCA-precipitated whole-cell extracts were separated by SDS-PAGE and analyzed by immunoblotting with anti-Myc and anti-Por1 antibodies. *B*, mitochondria (50 μg) isolated from WT and *coa2*Δ cells were solubilized with 1% digitonin and subjected to BN-PAGE. The distribution of 13xMyc epitope-tagged Oma1 and monomeric respiratory complex V (loading control) was assessed using anti-Myc antibodies and anti-F_1 serum, respectively. *C*, lysates obtained from 0.3 mg of either WT or *coa2*Δ mitochondria expressing Oma1–13Myc were separated by native electrophoresis in the first dimension and SDS-PAGE in the second dimension and analyzed by Western blotting with antibodies against Myc epitope. *Oma1^X* denotes the second species. *D*, *OMA1*::13Myc WT cells were grown to mid-logarithmic phase, diluted with the fresh culture medium, and incubated for an additional 2 h in the presence (+) or absence (−) of 6 mM H_2O_2 for 2 h at 30 °C. Mitochondria isolated from the respective cultures were analyzed by BN-PAGE as described above. *E*, steady-state levels of the indicated proteins were assessed in mitochondria derived from hydrogen peroxide-treated (+) and untreated (−) cells. *F*, two-dimensional BN-PAGE/SDS-PAGE analysis of *OMA1*::13Myc WT mitochondria isolated from the cells described in *D* and *E* was performed as described in Fig. 4*C*. *V*, complex V.

proteolytic activity and conversion of the high mass complex, we predicted that Oma1 was proteolytically active in *cox11*Δ cells. In support of this, membranes derived from *cox11*Δ mitochondria exhibited elevated Oma1-dependent proteolysis of FITC-casein (data not shown). However, Cox1 is not degraded in *cox11*Δ cells to the same extent as in *coa2*Δ cells (Figs. 2*A* and 3). Thus, these studies suggest that the facile Oma1-mediated degradation of Cox1 seen in *coa2*Δ cells may correlate with a proteolytic susceptible conformer of Cox1 uniquely found in these cells.

*Overexpression of Mitochondrial Chaperone Mdj1 Ameliorates Respiratory Defect in coa2*Δ *Cells*—The folding of Cox1 is likely impaired in *coa2*Δ cells leading to a misfolded conformer that is an efficient substrate for Oma1. We tested whether respiratory growth of *coa2*Δ cells was enhanced by overexpression of the mitochondrial Hsp70 chaperone Ssc1 or DnaJ protein Mdj1. High levels of Mdj1 gave a modest enhancement in growth of *coa2*Δ cells on glycerol/lactate (Fig. 7*E*). Overexpression of Ssc1 did not enhance any growth of *coa2*Δ cells on glyc-

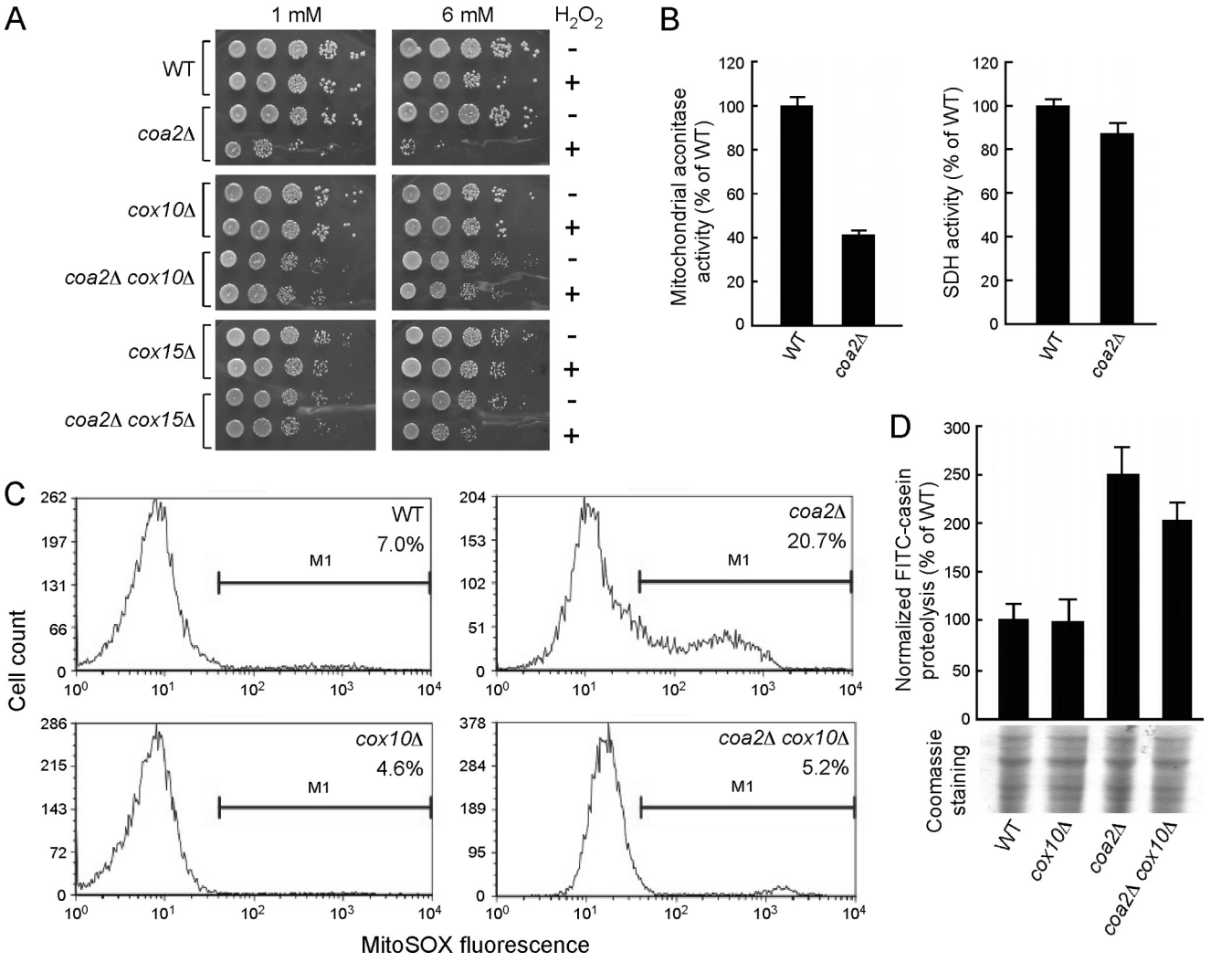

FIGURE 6. **Block of heme *a* synthesis in *coa2*Δ cells lowers reactive oxygen species (*ROS*) levels and proteolytic activity of mitochondrial membranes.** *A*, cells were grown to mid-logarithmic phase and incubated with (+) or without (−) the 6 mM H_2O_2 for 2 h at 30 °C. Following incubation, the samples were serially diluted and plated onto the complete medium with 2% glucose. Plates were incubated for 36–48 h at 30 °C. *B*, enzymatic activities of mitochondrial aconitase (*left panel*) and succinate dehydrogenase (*SDH*, *right panel*) in mitochondria isolated from WT and *coa2*Δ cells. Activities are shown as a percentage of the WT activity. The data represent an average of three biological replicates, and the *error bars* indicate S.D. *C*, flow cytometric analysis of endogenous reactive oxygen species in WT, *coa2*Δ, *cox10*Δ, and *coa2*Δ*cox10*Δ cultures stained with 5 μM MitoSox after 24 h of cultivation. The *x* axis on each panel indicates a log scale of the MitoSox fluorescence intensity, and the *y* axis represents cell counts. Any fluorescence outside of the gated area is indistinguishable from background and was not considered. The percentage of the cells within the gated area is indicated. *D*, proteolytic activities of the membranes from the strains listed above were tested as described in Fig. 3*A*.

erol/lactate (data not shown). To assess whether increasing Cox1 synthesis would augment the Mdj1-mediated enhancement in respiratory growth, we tested the effects of co-overexpression of Mdj1 and Mss51 (Fig. 7*E*). No synergistic effect was observed. The respiratory deficiency of *coa2*Δ cells persists even with elevated levels of newly synthesized Cox1 and the protein chaperone Mdj1. Therefore, neither Mdj1 nor Ssc1 are efficient chaperones of the misfolded Cox1 in the mutant cells.

DISCUSSION

Oma1 is shown presently to be a dominant protein that mediates the degradation of Cox1 specifically in *coa2*Δ cells. Depletion of Oma1, but not the mAAA protease, leads to a selective enrichment in newly synthesized Cox1 in *coa2*Δ cells but not other CcO assembly mutants. We previously demonstrated that the respiratory defect of *coa2*Δ cells was reversed by the depletion of the Oma1 protease, but the specificity of Oma1 in Cox1 degradation was not addressed. In the present work, we focus on the substrate specificity of Oma1 in the degradation of mitochondrially synthesized component of CcO and the bc_1 complex. In mutant strains stalled in CcO or bc_1 assembly, Oma1 did not appear to have any appreciable role in subunit degradation apart from *coa2*Δ cells. Oma1 appears to be activated in *coa2*Δ cells and other CcO assembly mutants such as *cox11*Δ cells. However, the facile Cox1 degradation observed in *coa2*Δ cells does not arise merely from Oma1 activation. The observed depletion of newly synthesized Cox1 may relate to the state of Cox1 as a proteolytic substrate in the mutant cells.

We previously reported that respiratory growth of *coa2*Δ cells is also restored by the presence of a gain-of-function allele of the Cox10 farnesyl transferase (19). We postulated that *coa2*Δ cells were impaired in Cox1 hemylation, and this defect

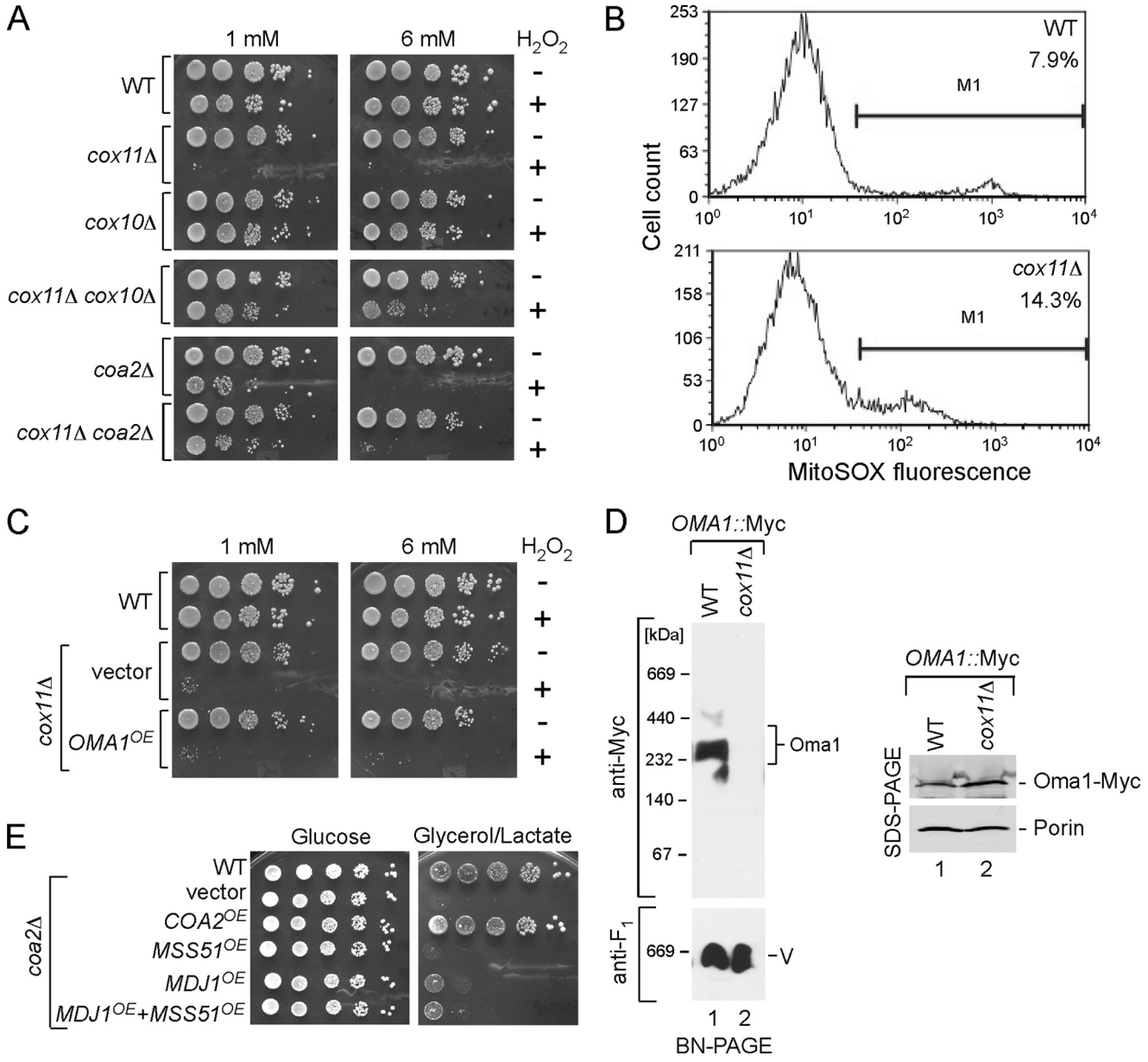

FIGURE 7. **Cells lacking Cox11 show oxidative stress and modulation of Oma1.** *A*, hydrogen peroxide sensitivity of indicated strains tested as in Fig. 6*A*. *B*, endogenous levels of reactive oxygen species in WT and *cox11*Δ cultures were analyzed by FACS as described in the legend to Fig. 6. *C*, sensitivity of either WT or *cox11*Δ cells transformed with an empty vector or Oma1-overexpressing plasmid. *D*, BN-PAGE (*left panel*) and SDS-PAGE (*right panel*) analyses of the Oma1-Myc complexes in the mitochondria isolated from WT or *cox11*Δ strains were carried out as described in the legend to Fig. 4. *E*, respiratory growth of the *coa2*Δ strain expressing Coa2, Mss51, Mdj1, or Mdj1 and Mss51. Cells were handled and tested as described in Fig. 1*A*. *V*, complex V.

could be suppressed by enhanced efficiency of hemylation by the mutant Cox10 enzyme or diminished proteolysis of the underhemylated Cox1. Impaired hemylation may result in a misfolded Cox1 that is a facile substrate for Oma1. The lack of an effect of Oma1 depletion in other CcO assembly mutants such as *cox11*Δ cells may relate to the population of the "heme *a*" subsite (as opposed to the heme a_3 subsite) in these mutants but not *coa2*Δ cells. Cox1 spans the IM with 12 TM helices organized in six successive helical pairs forming a closed bundle (1). The farnesyl tail of the heme *a* in the heme *a* subsite is packed between helices 1, 11, and 12. The axial His ligands for heme *a* ligation come from His-62 in helix 2 and His-378 in helix 10. Thus, heme *a* binding in the *a* subsite is expected to stabilize the Cox1 helical bundle. The a_3 subsite heme *a* does not appear to have the same stabilizing role. Thus, failure to hemylate the *a* subsite may be expected to destabilize Cox1 leading to rapid degradation. Coa2 is predicted to have a specialized role in mediating the population of the heme *a* subsite. Coa2 may be a Cox1 chaperone stabilizing a conformer competent for heme *a* insertion.

Two forms of non-hemylated Cox1 are not substrates of Oma1. First, the initial newly synthesized Cox1 complex containing Mss51, Cox14, Coa3, and Ssc1 persists in *coa2*Δ cells (18). The presence of the three CcO assembly factors in addition to the Ssc1 chaperone may stabilize Cox1 within this non-hemylated complex against rapid degradation. These proteins may protect the C-terminal segment of Cox1 that is matrix facing where the Oma1 catalytic site appears to be localized.

Second, cells lacking Cox14 or Mss51 fail to form the Mss51 complex yet still do not show an Oma1-dependence in Cox1 degradation. Oma1 may not be fully active in *cox14*Δ or *mss51*Δ cells due to the lack of Cox10 activation (19). The rapid turnover of Cox1 in *coa2*Δ cells appears to arise from both the impaired hemylation of Cox1 and the heme *a*-mediated stress to activate Oma1.

The specificity of Oma1 for Cox1 degradation in *coa2*Δ cells is curious because iAAA and mAAA proteases are known to degrade misfolded mitochondrial proteins. Misfolded Cox1 in *coa2*Δ cells may exist within a particular subdomain of the mitochondrial IM accessible to Oma1 but not the ATP proteases. Alternatively, Oma1 may be important for initial cleavage and final proteolysis may be subsequently mediated by the AAA proteases. The recent cryo-EM reconstruction of the mAAA protease suggests that entry of a protein into the AAA hexameric ring may be restricted to unfolded polypeptide segments (39). Oma1 may function to generate a more unfolded state that can be accommodated by one of the AAA proteases.

Oma1 is one of the mitochondrial proteases important in removing misfolded mitochondrial proteins. Yeast Oma1 was shown to be involved in the cleavage of the artificially misfolded polytopic IM protein Oxa1 (35). In mammalian cells, Oma1 functions in conjuction with the mAAA protease in stress-triggered processing of OPA1, a GTPase involved in mitochondrial membrane dynamics and genome maintenance (40, 41).

Oma1 activation was reported to occur in conditions in which mammalian mitochondria are dysfunctional (40, 41). Oma1 was reported to be proteolyzed within functional mitochondria precluding its function. Dissipation of the mitochondrial membrane potential blocked Oma1 cleavage thereby stabilizing the active state. We show presently that Oma1 is not regulated by proteolysis in yeast. Oma1 may be activated in cells with an impaired membrane potential through another mechanism such as protein modification. Oma1 was postulated to form a homohexameric structure that is independent of ATP (35). The observed change in mobility of the Oma1 complex in respiratory deficient or stressed mitochondria may relate to a change in the conformation or composition of the protein complex. Future studies will focus on the elucidation of the functional states and activation process of Oma1.

Acknowledgments—We thank Dr. T. Langer for the YMN503 strain defective in the mAAA protease and YTA10 plasmids, Dr. X. Pérez Martínez for the Cox1ΔC15 strain, and Dr. B. Trumpower for the qcr7 null strain. We acknowledge the assistance of the Flow Cytometry core facility at the University of Utah Health Sciences Center.

REFERENCES

1. Tsukihara, T., Aoyama, H., Yamashita, E., Tomizaki, T., Yamaguchi, H., Shinzawa-Itoh, K., Nakashima, R., Yaono, R., and Yoshikawa, S. (1995) Structures of metal sites of oxidized bovine heart cytochrome *c* oxidase at 2.8 A. *Science* **269,** 1069–1074
2. Tsukihara, T., Aoyama, H., Yamashita, E., Tomizaki, T., Yamaguchi, H., Shinzawa-Itoh, K., Nakashima, R., Yaono, R., and Yoshikawa, S. (1996) The whole structure of the 13-subunit oxidized cytochrome *c* oxidase at 2.8 A. *Science* **272,** 1136–1144
3. Heinemeyer, J., Braun, H. P., Boekema, E. J., and Kouril, R. (2007) A structural model of the cytochrome *c* reductase/oxidase supercomplex from yeast mitochondria. *J. Biol. Chem.* **282,** 12240–12248
4. Manthey, G. M., and McEwen, J. E. (1995) The product of the nuclear gene PET309 is required for translation of mature mRNA and stability or production of intron-containing RNAs derived from the mitochondrial COX1 locus of *Saccharomyces cerevisiae*. *EMBO J.* **14,** 4031–4043
5. Manthey, G. M., Przybyla-Zawislak, B. D., and McEwen, J. E. (1998) The *Saccharomyces cerevisiae* Pet309 protein is embedded in the mitochondrial inner membrane. *Eur. J. Biochem.* **255,** 156–161
6. Siep, M., van Oosterum, K., Neufeglise, H., van der Spek, H., and Grivell, L. A. (2000) Mss51p, a putative translational activator of cytochrome *c* oxidase subunit-1 (COX1) mRNA, is required for synthesis of Cox1p in *Saccharomyces cerevisiae*. *Curr. Genet.* **37,** 213–220
7. Perez-Martinez, X., Broadley, S. A., and Fox, T. D. (2003) Mss51p promotes mitochondrial Cox1p synthesis and interacts with newly synthesized Cox1p. *EMBO J.* **22,** 5951–5961
8. Bonnefoy, N., Chalvet, F., Hamel, P., Slonimski, P. P., and Dujardin, G. (1994) OXA1, a *Saccharomyces cerevisiae* nuclear gene whose sequence is conserved from prokaryotes to eukaryotes controls cytochrome oxidase biogenesis. *J. Mol. Biol.* **239,** 201–212
9. Hell, K., Neupert, W., and Stuart, R. A. (2001) Oxa1p acts as a general membrane insertion machinery for proteins encoded by mitochondrial DNA. *EMBO J.* **20,** 1281–1288
10. Barrientos, A., Zambrano, A., and Tzagoloff, A. (2004) Mss51p and Cox14p jointly regulate mitochondrial Cox1p expression in *Saccharomyces cerevisiae*. *EMBO J.* **23,** 3472–3482
11. Pierrel, F., Bestwick, M. L., Cobine, P. A., Khalimonchuk, O., Cricco, J. A., and Winge, D. R. (2007) Coa1 links the Mss51 post-translational function to Cox1 cofactor insertion in cytochrome *c* oxidase assembly. *EMBO J.* **26,** 4335–4346
12. Mick, D. U., Vukotic, M., Piechura, H., Meyer, H. E., Warscheid, B., Deckers, M., and Rehling, P. (2010) Coa3 and Cox14 are essential for negative feedback regulation of COX1 translation in mitochondria. *J. Cell Biol.* **191,** 141–154
13. Fontanesi, F., Soto, I. C., Horn, D., and Barrientos, A. (2010) Mss51 and Ssc1 facilitate translational regulation of cytochrome *c* oxidase biogenesis. *Mol. Cell. Biol.* **30,** 245–259
14. Mick, D. U., Wagner, K., van der Laan, M., Frazier, A. E., Perschil, I., Pawlas, M., Meyer, H. E., Warscheid, B., and Rehling, P. (2007) Shy1 couples Cox1 translational regulation to cytochrome *c* oxidase assembly. *EMBO J.* **26,** 4347–4358
15. Shingú-Vázquez, M., Camacho-Villasana, Y., Sandoval-Romero, L., Butler, C. A., Fox, T. D., and Pérez-Martínez, X. (2010) The carboxyl-terminal end of Cox1 is required for feedback assembly regulation of Cox1 synthesis in *Saccharomyces cerevisiae* mitochondria. *J. Biol. Chem.* **285,** 34382–34389
16. Khalimonchuk, O., Bestwick, M., Meunier, B., Watts, T. C., and Winge, D. R. (2010) Formation of the redox cofactor centers during Cox1 maturation in yeast cytochrome oxidase. *Mol. Cell. Biol.* **30,** 1004–1017
17. Glerum, D. M., and Tzagoloff, A. (1994) Isolation of a human cDNA for heme A:farnesyltransferase by functional complementation of a yeast cox10 mutant. *Proc. Natl. Acad. Sci. U.S.A.* **91,** 8452–8456
18. Pierrel, F., Khalimonchuk, O., Cobine, P. A., Bestwick, M., and Winge, D. R. (2008) Coa2 is an assembly factor for yeast cytochrome *c* oxidase biogenesis that facilitates the maturation of Cox1. *Mol. Cell. Biol.* **28,** 4927–4939
19. Bestwick, M., Khalimonchuk, O., Pierrel, F., and Winge, D. R. (2010) The role of Coa2 in hemylation of yeast Cox1 revealed by its genetic interaction with Cox10. *Mol. Cell. Biol.* **30,** 172–185
20. Wang, Z., Wang, Y., and Hegg, E. L. (2009) Regulation of the heme A biosynthetic pathway: Differential regulation of heme A synthase and heme O synthase in *Saccharomyces cerevisiae*. *J. Biol. Chem.* **284,** 839–847
21. Wang, F., Song, W., Brancati, G., and Segatori, L. (2011) Inhibition of endoplasmic reticulum-associated degradation rescues native folding in loss of function protein misfolding diseases. *J. Biol. Chem.* **286,** 43454–43464
22. Sambrook, J., Fritsch, E. F., and Mantiatis, T. (1989) *Molecular cloning: A laboratory manual*, Cold Spring Harbor Laboratory Press, Cold Spring

Harbor, New York
23. Schiestl, R. H., and Gietz, R. D. (1989) High efficiency transformation of intact yeast cells using single stranded nucleic acids as a carrier. *Curr. Genet.* **16,** 339–346
24. Khalimonchuk, O., Bird, A., and Winge, D. R. (2007) Evidence for a pro-oxidant intermediate in the assembly of cytochrome oxidase. *J. Biol. Chem.* **282,** 17442–17449
25. Daum, G., Böhni, P. C., and Schatz, G. (1982) Import of proteins into mitochondria. Cytochrome b2 and cytochrome *c* peroxidase are located in the intermembrane space of yeast mitochondria. *J. Biol. Chem.* **257,** 13028–13033
26. Bradford, M. M. (1976) A rapid and sensitive method for the quantitation of microgram quantities of protein utilizing the principle of protein dye binding. *Anal. Biochem.* **72,** 248–254
27. Capaldi, R. A., Marusich, M. F., and Taanman, J. W. (1995) Mammalian cytochrome *c* oxidase: Characterization of enzyme and immunological detection of subunits in tissue extracts and whole cells. *Methods Enzymol.* **260,** 117–132
28. Oyedotun, K. S., and Lemire, B. D. (2004) The quaternary structure of the *Saccharomyces cerevisiae* succinate dehydrogenase. Homology modeling, cofactor docking, and molecular dynamics simulation studies. *J. Biol. Chem.* **279,** 9424–9431
29. Gardner, P. R., Nguyen, D. D., and White, C. W. (1994) Aconitase is a sensitive and critical target of oxygen poisoning in cultured mammalian cells and in rat lungs. *Proc. Natl. Acad. Sci. U.S.A.* **91,** 12248–12252
30. Bulteau, A. L., Dancis, A., Gareil, M., Montagne, J. J., Camadro, J. M., and Lesuisse, E. (2007) Oxidative stress and protease dysfunction in the yeast model of Friedreich ataxia. *Free Rad. Biol. Med.* **42,** 1561–1570
31. Barrientos, A., Korr, D., and Tzagoloff, A. (2002) Shy1p is necessary for full expression of mitochondrial COX1 in the yeast model of Leigh syndrome. *EMBO J.* **21,** 43–52
32. Nolden, M., Ehses, S., Koppen, M., Bernacchia, A., Rugarli, E. I., and Langer, T. (2005) The m-AAA protease defective in hereditary spastic paraplegia controls ribosome assembly in mitochondria. *Cell* **123,** 277–289
33. Zara, V., Palmisano, I., Conte, L., and Trumpower, B. L. (2004) *Eur. J. Biochem.* **271,** 1209–1218
34. Savel'ev, A. S., Novikova, L. A., Kovaleva, I. E., Luzikov, V. N., Neupert, W., and Langer, T. (1998) ATP-dependent proteolysis in mitochondria. m-AAA protease and PIM1 protease exert overlapping substrate specificities and cooperate with the mtHsp70 system. *J. Biol. Chem.* **273,** 20596–20602
35. Kaser, M., Kambacheld, M., Kisters-Woike, B., and Langer, T. (2003) Oma1, a novel membrane-bound metallopeptidase in mitochondria with activities overlapping with the m-AAA protease. *J. Biol. Chem.* **278,** 46414–46423
36. Pain, J., Balamurali, M. M., Dancis, A., and Pain, D. (2010) Mitochondrial NADH kinase, Pos5p, is required for efficient iron-sulfur cluster biogenesis in *Saccharomyces cerevisiae*. *J. Biol. Chem.* **285,** 39409–39424
37. Dickinson, B. C., Srikun, D., and Chang, C. J. (2010) Mitochondrial-targeted fluorescent probes for reactive oxygen species. *Curr. Opin. Chem. Biol.* **14,** 50–56
38. Hiser, L., Di Valentin, M., Hamer, A. G., and Hosler, J. P. (2000) Cox11p is required for stable formation of the Cu(B) and magnesium centers of cytochrome *c* oxidase. *J. Biol. Chem.* **275,** 619–623
39. Lee, S., Augustin, S., Tatsuta, T., Gerdes, F., Langer, T., and Tsai, F. T. (2011) Electron cryomicroscopy structure of a membrane-anchored mitochondrial AAA protease. *J. Biol. Chem.* **286,** 4404–4411
40. Ehses, S., Raschke, I., Mancuso, G., Bernacchia, A., Geimer, S., Tondera, D., Martinou, J. C., Westermann, B., Rugarli, E. I., and Langer, T. (2009) Regulation of OPA1 processing and mitochondrial fusion by m-AAA protease isoenzymes and OMA1. *J. Cell Biol.* **187,** 1023–1036
41. Head, B., Griparic, L., Amiri, M., Gandre-Babbe, S., and van der Bliek, A. M. (2009) Inducible proteolytic inactivation of OPA1 mediated by the OMA1 protease in mammalian cells. *J. Cell Biol.* **187,** 959–966